ON THE DESIGN AND USE OF ONCE-DIFFERENTIABLE HIGH DYNAMIC RESOLUTION ATOMS FOR THE DISTRIBUTION DERIVATIVE METHOD

Nicholas Esterer

SPCL*
McGill University
Montreal, Quebec, Canada
nicholas.esterer@mail.mcgill.ca

Philippe Depalle

SPCL
McGill University
Montreal, Quebec, Canada
philippe.depalle@mcgill.ca

ABSTRACT

The accuracy of the Distribution Derivative Method (DDM) [1] is evaluated on mixtures of chirp signals. It is shown that accurate estimation can be obtained when the sets of atoms for which the inner product is large are disjoint. This amounts to designing atoms with windows whose Fourier transform exhibits low sidelobes but which are once-differentiable in the time-domain. A technique for designing once-differentiable approximations to windows is presented and the accuracy of these windows in estimating the parameters of sinusoidal chirps in mixture is evaluated.

1. INTRODUCTION

Additive synthesis using a sum of sinusoids plus noise is a powerful model for representing audio [2], allowing for the easy implementation of many manipulations such as time-stretching [3] and timbre-morphing [4]. In these papers, [2–4] the phase evolution of the sinusoid is assumed linear over the analysis frame, only the phase and frequency of the sinusoids at these analysis points are used to fit a plausible phase function after some the analysis points are connected to form a partial [5]. Recently, there has been interest in using higher-order phase functions [6] as the estimation of their parameters has been made possible by a new set of techniques of only moderate computational complexity using signal derivatives [7]. The use of higher-order phase models allows for accurate description of highly modulated signals, for example in the analysis of birdsong [8]. The frequency modulation information has also been used in the regularization of mathematical programs for audio source separation [9].

The sinusoidal model approximating signal s typically considered is

$$\tilde{s}(t) = \exp(a_0 + \sum_{q=1}^{Q} a_q t^q) + \eta(t) \tag{1}$$

where $\tilde{s}$ is the approximating signal, t the variable of time, the $a_q \in \mathbb{C}$ coefficients of the argument's polynomial, and $\eta(t)$ white Gaussian noise. Although this technique can be extended to describe a single sinusoid of arbitrary complexity simply by increasing Q, it remains essential to consider signals featuring a sum of P such components, whether they represent the harmonic structure of a musical sound or the union of partials resulting from a mixture of multiple signal sources (e.g., recordings of multiple speakers or performers), i.e.,

$$x(t) = \sum_{p=1}^{P} x_p(t) + \eta(t) \tag{2}$$

with

$$x_p(t) = \exp(a_{p,0} + \sum_{q=1}^{Q} a_{p,q} t^q) \tag{3}$$

As regards the design and evaluation of signal-derivatives analysis techniques, previous work has generally assumed signals containing a single component, i.e., $P = 1$ or assumed the influence of other components to be negligible. Later we will refine when this assumption can be made. In [10] the authors provide a comprehensive evaluation of various signal-derivatives analysis methods applied to a single-component signal. In [11] the extent to which two components in mixture can corrupt estimations of the frequency slope ($\Im\{a_{0,2}\}$ and $\Im\{a_{1,2}\}$) is investigated in the context of the reassignment method, one of the signal-derivatives techniques, but the corruption of the other parameters is not considered.

In this paper, we revisit the quality of signal-derivatives estimation of *all* the a_q when analyzing a *mixture* of components. We focus on the DDM [1] analysis method for its convenience as it can simply be considered as an atomic decomposition (see Sec. 2), and does not require computing derivatives of the signal to be analysed.

The DDM does, however, require a once-differentiable analysis window. As we are interested in windows with lower sidelobes in order to better estimate parameters of sinusoidal chirp signals in mixture, we seek windows that combine these two properties. For this, a technique to design once-differentiable approximations to arbitrary symmetrical windows is proposed and presented along with a design example for a high-performance window. Finally we evaluate the performance of various once-differentiable windows in estimating the parameters a_q.

2. ESTIMATING THE PARAMETERS a_q

We will now show briefly how the DDM can be used to estimate the a_q. Based on the theory of distributions [12], the DDM makes use of "test functions" or atoms ψ. These atoms must be once differentiable with respect to time variable t and be non-zero only on a finite interval $[-\frac{L_t}{2}, \frac{L_t}{2}]$. First, we define the inner product

$$\langle x, \psi \rangle = \int_{-\infty}^{\infty} x(t)\overline{\psi}(t)dt \tag{4}$$

and the operator

$$\mathcal{T}^\alpha : (\mathcal{T}^\alpha x)(t) = t^\alpha x(t) \tag{5}$$

Consider the weighted signal

$$f(t) = x(t)\overline{\psi}(t) \tag{6}$$

* Sound Processing and Control Laboratory

differentiating with respect to t we obtain

$$\frac{df}{dt}(t) = \frac{dx}{dt}(t)\overline{\psi}(t) + x(t)\frac{d\overline{\psi}}{dt}(t) = \left(\sum_{q=1}^{Q} q a_q t^{q-1}\right) x(t)\overline{\psi}(t) + x(t)\frac{d\overline{\psi}}{dt}(t) \quad (7)$$

Because ψ is zero outside of the interval $[-\frac{L_t}{2}, \frac{L_t}{2}]$, integrating $\frac{df}{dt}(t)$ we obtain

$$\int_{-\infty}^{\infty} \frac{df}{dt}(t)dt = \sum_{q=1}^{Q} q a_q \int_{-\frac{L_t}{2}}^{\frac{L_t}{2}} t^{q-1} x(t)\overline{\psi}(t)dt + \left\langle x, \frac{d\overline{\psi}}{dt} \right\rangle = 0 \quad (8)$$

or, using the operator $\mathcal{T}^\alpha$,

$$\sum_{q=1}^{Q} q a_q \left\langle \mathcal{T}^{q-1} x, \overline{\psi} \right\rangle = -\left\langle x, \frac{d\overline{\psi}}{dt} \right\rangle \quad (9)$$

Estimating coefficients a_q, $1 < q \leq Q$, simply requires R atoms ψ_r with $R \geq Q$ to solve the linear system of equations

$$\sum_{q=1}^{Q} q a_q \left\langle \mathcal{T}^{q-1} x, \overline{\psi}_r \right\rangle = -\left\langle x, \frac{d\overline{\psi}_r}{dt} \right\rangle \quad (10)$$

for $1 \leq r \leq R$.

To estimate a_0 we rewrite the signal we are analysing as

$$x(t) = \exp(a_0)\gamma(t) + \epsilon(t) \quad (11)$$

where $\epsilon(t)$ is the error signal, the part of the signal that is not explained by our model, and $\gamma(t)$ is the part of the signal whose coefficients have already been estimated, i.e.,

$$\gamma(t) = \exp\left(\sum_{q=1}^{Q} a_q t^q\right) \quad (12)$$

Computing the inner product $\langle x, \gamma \rangle$, we have

$$\langle x, \gamma \rangle = \langle \exp(a_0)\gamma, \gamma \rangle + \langle \epsilon, \gamma \rangle \quad (13)$$

The inner product between ϵ and γ is 0, by the orthogonality principle [13, ch. 12]. Furthermore, because $\exp(a_0)$ does not depend on t, we have

$$\langle x, \gamma \rangle = \exp(a_0) \langle \gamma, \gamma \rangle \quad (14)$$

so we can estimate a_0 as

$$a_0 = \log\left(\langle x, \gamma \rangle\right) - \log\left(\langle \gamma, \gamma \rangle\right) \quad (15)$$

As will be seen in subsequent sections, the DDM typically involves taking the discrete Fourier transform (DFT) of the signal windowed by both an everywhere once-differentiable function of finite support (e.g., the Hann window) and this function's derivative. A small subset of atoms corresponding to the peak bins in the DFT are used in Eq. 10 to solve for the parameters a_q.

3. ESTIMATING THE $a_{p,q}$ OF P COMPONENTS

We examine how the mixture model influences the estimation of the $a_{p,q}$ in Eq. 3. Consider a mixture of P components. If we define the weighted signal sum

$$g(t) = \sum_{p=1}^{P} x_p(t)\overline{\psi}(t) = \sum_{p=1}^{P} f_p(t) \quad (16)$$

and substitute g for f in Eq. 7 we obtain

$$\sum_{p=1}^{P} \int_{-\frac{L_t}{2}}^{\frac{L_t}{2}} \frac{df_p}{dt}(t)dt = 0 = \sum_{p=1}^{P} \left(\sum_{q=1}^{Q} q a_{p,q} \left\langle \mathcal{T}^{q-1} x_p, \overline{\psi} \right\rangle + \left\langle x_p, \frac{d\overline{\psi}}{dt} \right\rangle \right) \quad (17)$$

From this we see if $\left\langle \mathcal{T}^{q-1} x_p, \overline{\psi}_r \right\rangle$ and $\left\langle x_p, \frac{d\overline{\psi}_r}{dt} \right\rangle$ are small for all but $p = p^*$ and a subset of R atoms[1], we can simply estimate the parameters $a_{p^*,q}$ using

$$\sum_{q=1}^{Q} q a_{p^*,q} \left\langle \mathcal{T}^{q-1} x_{p^*}, \overline{\psi}_r \right\rangle = -\left\langle x_{p^*}, \frac{d\overline{\psi}_r}{dn} \right\rangle \quad (18)$$

for $1 \leq r \leq R$. To compute $a_{p^*,0}$ we simply use

$$\gamma_{p^*}(t) = \exp\left(\sum_{q=1}^{Q} a_{p^*,q} t^q\right) \quad (19)$$

in place of γ in Eq. 15.

4. DESIGNING THE ψ_R

In practice, an approximation of Eq. 4 is evaluated using the DFT on a signal x that is properly sampled and so can be evaluated at a finite number of times nT with $n \in [0, N-1]$ and T the sample period in seconds. In this way, the chosen atoms $\psi_\omega(t)$ are the products of the elements of the Fourier basis and an appropriately chosen window w that is once differentiable and finite, i.e.,

$$\psi_\omega(t) = w(t)\exp(-j\omega t) \quad (20)$$

Defining $N = \frac{L_t}{T}$ and angular frequency at bin r as $\omega_r = 2\pi\frac{r}{N}$, the approximate inner product is then

$$\langle x, \psi_\omega \rangle \approx \sum_{n=0}^{N-1} x(Tn)w(Tn)\exp(-2\pi j r\frac{n}{N}) \quad (21)$$

i.e., the definition of the DFT of a windowed signal[2]. The DFT is readily interpreted as a bank of bandpass filters centred at normalized frequencies $\frac{r}{N}$ and with frequency response described by

[1] The notation x^* will mean the value of the argument x maximizing or minimizing some function.

[2] Notice however that this is an approximation of the inner product and should not be interpreted as yielding the Fourier series coefficients of a properly sampled signal x periodic in L_t. This means that other evaluations of the inner product that yield more accurate results are possible. For example, the analytic solution is possible if x is assumed zero outside of $[-\frac{L_t}{2}, \frac{L_t}{2}]$ (the ψ are in general analytic). In this case the samples of x are convolved with the appropriate interpolating sinc functions and the integral of this function's product with ψ is evaluated.

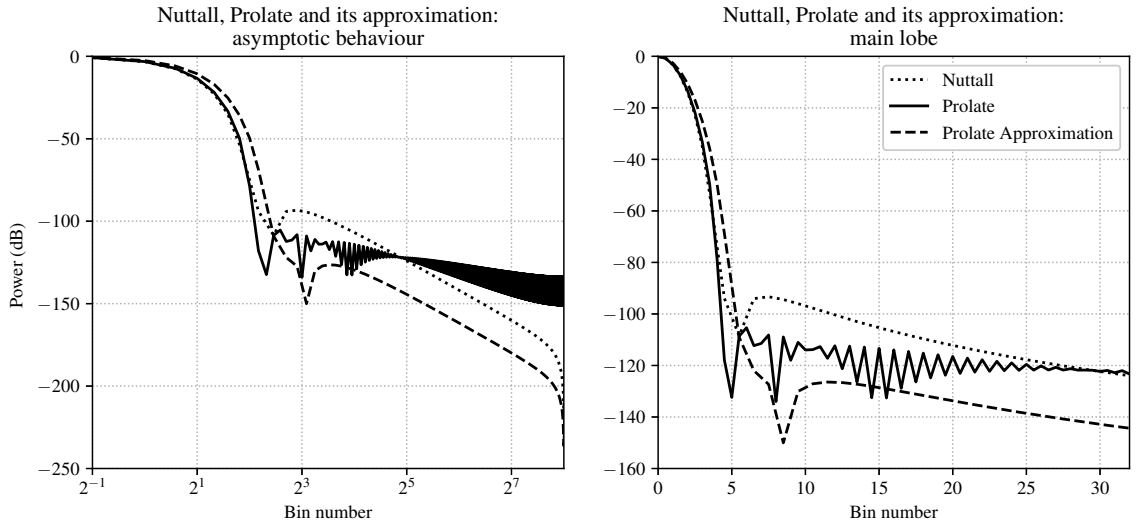

Figure 1: Comparing the main-lobe and asymptotic power spectrum characteristics of the continuous 4-term Nuttall window, the digital prolate window with $W = 0.008$, and the continuous approximation to the digital prolate window.

the Fourier transform of modulated w [14]. Therefore choosing ψ amounts to a filter design problem under the constraints that the impulse response of the filter be differentiable in t and finite. To minimize the influence of all but one component, granted the components's energy concentrations are sufficiently separated in frequency, we desire impulse responses whose magnitude response gives maximum out-of-band rejection or equivalently, windows whose Fourier transform exhibits the lowest sidelobes.

In all the publications reviewed on the DDM for this paper, the window used was the Hann window which is once-differentiable everywhere in the time-domain. In [11], a publication on the reassignment method, other windows than the Hann are considered but these windows must be twice-differentiable. Nuttall [15] has designed windows with lower sidelobes than the canonical Hann window which are everywhere at least once-differentiable. It is also possible to design approximations to arbitrary symmetrical window functions using harmonically related cosines, as is discussed in the following section.

5. DIFFERENTIABLE APPROXIMATIONS TO WINDOWS

A differentiable approximation to a symmetrical window can be designed in a straightforward way. In [16] and [17] it is shown how to design optimal windows of length N samples using a linear combination of M harmonically related cosines

$$\tilde{w}(n) = \sum_{m=0}^{M-1} b_m \cos(2\pi m \frac{n}{N}) \mathcal{R}(\frac{n}{N}) \tag{22}$$

where $\mathcal{R}$ is the *rectangle function*. This function is discontinuous at $n = \frac{\pm N}{2}$, and therefore not differentiable there, unless

$$\sum_{m=0}^{M-1} b_m \cos(\pm \pi m) = 0 \tag{23}$$

Rather than design based on an optimality criterion, such as the height of the highest sidelobe [17], a once-differentiable approximation to an existing window w is desired. To do this, we choose the b_m so that the window $\tilde{w}$'s squared approximation error to w is minimized while having $\tilde{w}(\frac{\pm N}{2}) = 0$, i.e. we find the solution $\{b_m^*\}$ to the mathematical program

$$\text{minimize} \sum_{n=0}^{N-1} (w(n) - \sum_{m=0}^{M-1} b_m \cos(2\pi m \frac{n}{N}))^2 \tag{24}$$

$$\text{subject to} \sum_{m=0}^{M-1} b_m \cos(\pi m) = 0 \tag{25}$$

which can be solved using constrained least-squares; a standard numerical linear algebra routine [18, p. 585].

6. A CONTINUOUS WINDOW DESIGN EXAMPLE

As a design example we show how to create a continuous approximation of a digital prolate spheroidal window.

Digital prolate spheroidal windows are a parametric approximation to functions whose Fourier transform's energy is maximized in a given bandwidth [19]. These can be tuned to have extremely low sidelobes, at the expense of main-lobe width. Differentiation of these window functions may be possible but is not as straightforward as differentiation of the sum-of-cosine windows above. Furthermore, the windows do not generally have end-points equal to 0. In the following we will demonstrate how to approximate a digital prolate spheroidal window with one that is everywhere at least once-differentiable.

In [20] it was shown how to construct digital prolate spheroidal windows under parameters N, the window length in samples, and a parameter W choosing the (normalized) frequency range in which the proportion of the main lobe's energy is to be maximized. We chose $N = 512$ based on the window length chosen in [1] for ease of comparison. Its W parameter's value was chosen by synthesizing windows with W ranging between 0.005 and 0.010 at a

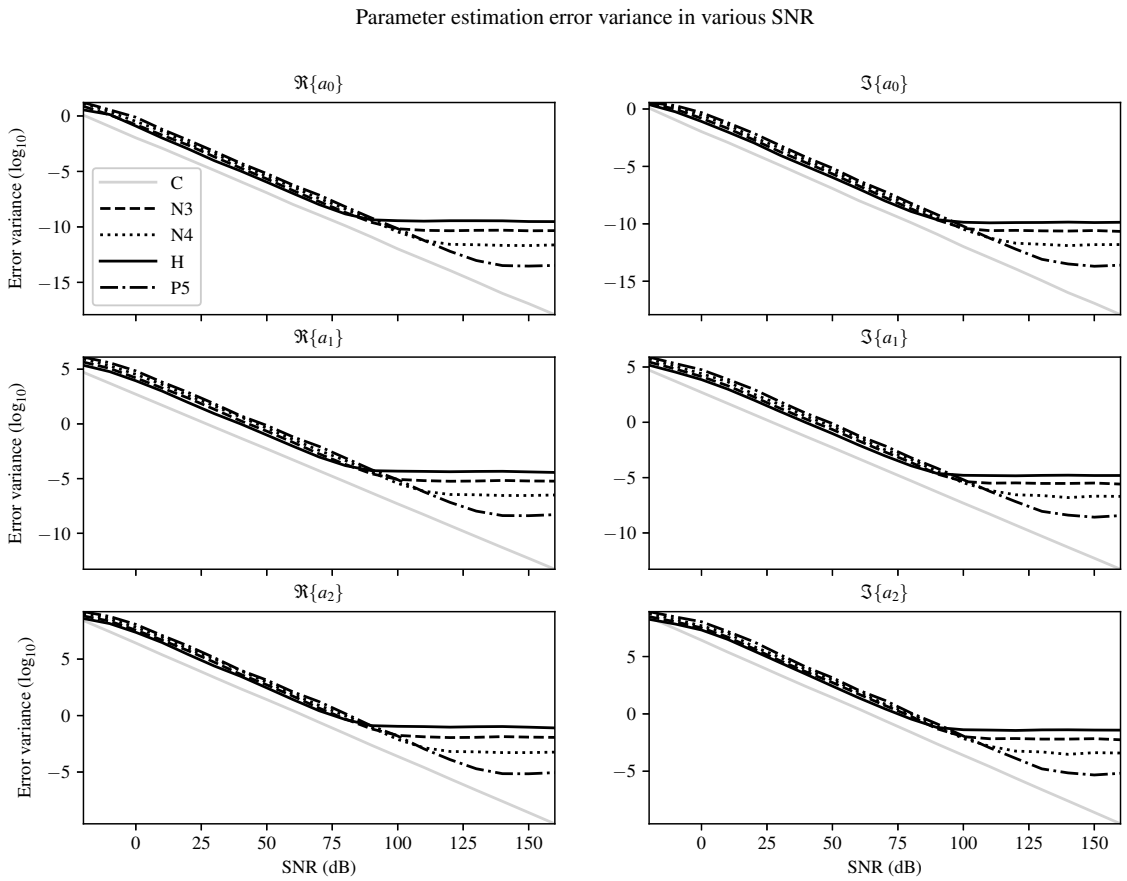

Figure 2: The estimation variance of random polynomial phase sinusoids averaged over $K_1 = 1000$ trials using atoms generated from various windows. *C* is the Cramér-Rao lower bound, *N3* and *N4* are the 3- and 4-cosine-term continuous Nuttall windows, *H* is the Hann window, and *P5* is the continuous 5-cosine-term approximation to a digital prolate window as described in Sec. 6.

Table 1: The coefficients of the once-differentiable approximation to a digital prolate window designed in Sec. 6.

$$\begin{aligned} b_0 &= 3.128 \times 10^{-1} \\ b_1 &= 4.655 \times 10^{-1} \\ b_2 &= 1.851 \times 10^{-1} \\ b_3 &= 3.446 \times 10^{-2} \\ b_4 &= 2.071 \times 10^{-3} \end{aligned}$$

resolution of 0.001. The window with the closest 3 dB bandwidth to the 4-term Nuttall window was obtained with $W = 0.008$. Its magnitude response is shown in Fig. 1. We see that this window's asymptotic falloff is 6 dB per octave and therefore has a discontinuity somewhere in its domain [15].

We designed an approximate window using Eq. 24 for M varying between 2 and $N/8$ to find the best approximation to the digital prolate window's main lobe using a small number of cosines. The M giving the best approximation was 5. The magnitude response of the approximation is shown in Fig. 1 and its coefficients are listed in Tab. 1; the temporal shape is very close to a digital prolate spheroidal window with $W = 0.008$ and is therefore omitted for brevity.

It is seen that a lower highest sidelobe level than the Nuttall and Prolate windows is obtained by slightly sacrificing the narrowness of the main lobe. More importantly, in Fig. 1 we observe that the falloff of the window is 18 dB per octave because it is once-differentiable at all points in its domain.

7. THE PERFORMANCE OF IMPROVED WINDOWS

7.1. Signals with single component

To compare the average estimation error variance with the theoretical minimum given by the Cramér-Rao bound we synthesized K_1 random chirps using Eq. 1 with $Q = 2$ and parameters chosen from uniform distributions justified in [1]. The original Hann window, the windows proposed by Nuttall and the new digital prolate based window were used to synthesize the atoms as described in Sec. 4 and their estimation error variance was compared (see Fig. 2). After performing the DFT to obtain inner products with the

atoms, the three atoms whose inner products were greatest were used in the estimations, i.e., $R = 3$ in Eq. 10. The windows with the lowest sidelobes only give the lowest error variance at very favourable SNRs, at real-world SNRs the original Hann window still performs best at estimating the parameters of a single component signal.

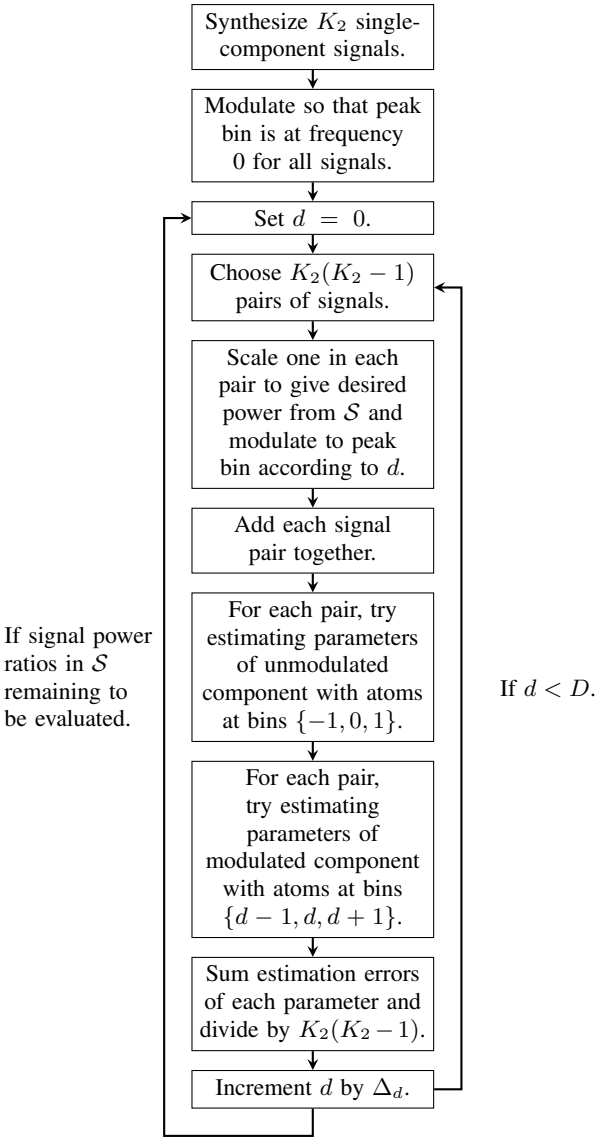

Figure 4: The evaluation procedure for 2-component signals.

7.2. Signals with 2 components

To evaluate the performance of the various windows when estimating the parameters of components in mixture we synthesized signals using Eq. 3 with $P = 2$ and $Q = 2$ and parameters chosen from the uniform distributions specified in [1]. We desired to see how the accuracy of estimation is influenced by the difference (in bins) between the locally maximized atoms and the difference in signal power between the two components. To obtain a set of components from which test signals exhibiting the desired differences could be constructed, we synthesized a set $\mathcal{C}$ of K_2 components for which the energy is maximized in bin 0. Test signals were obtained by choosing a pair of unique components from this set and modulating one to give the desired frequency and amplitude difference. This was carried out as follows: the atom r^* for which the inner product was maximized was determined for each unmixed chirp and the chirp was modulated by $\exp(-2\pi \frac{r^* n}{N} j)$ for $0 \leq n < N$ in order to move this maximum to $r = 0$. Then for each desired difference d, with $0 \leq d < D$ (for the evaluation $D = 40$), two unique chirps were selected from $\mathcal{C}$ and one chirp was modulated by $\exp(2\pi \frac{nd}{N} j)$ for $0 \leq n < N$ in order to give the desired difference between maxima. This component was also scaled by a constant to give a desired signal power ratio from set $\mathcal{S}$ with the other component (the power ratios $\mathcal{S}$ tested were 0 dB and -30 dB). As we assume perfect peak-atom selection for this evaluation no inner-product maximizing r^* is chosen, rather atoms with angular frequencies $\omega = 2\pi \frac{\hat{d}}{N}$ for $\hat{d} \in \{d-1, d, d+1\}$ in Eq. 20 (again, $R = 3$) were chosen to carry out the estimation. d was incremented by $\Delta_d = 0.25$ and so $\hat{d}$ was not generally integral valued in this case. The parameters of the unmodulated component were estimated using angular frequencies $\omega = 2\pi \frac{\hat{d}}{N}$ for $\hat{d} \in \{-1, 0, 1\}$ in Eq. 20. The squared estimation error for each parameter was summed and divided by $K_2(K_2-1)$ (the number of choices of two unique components) to give the averaged squared estimation error for each parameter at each difference d. The procedure is summarized in Fig. 4.

The behaviour of the windows when used to analyse mixtures of non-stationary signals is similar to the behaviour of windows used for harmonic analysis in the stationary case [16]; here we obtain further insight into how the estimation of each coefficient of the polynomial in Eq. 1 is influenced by main-lobe width and sidelobe height and slope. In Fig. 3 we see that there is generally less estimation error for components having similar signal power. This is to be expected as there will be less masking of the weaker signal in these scenarios. The estimation error is large when the atoms containing the most signal energy for each component are not greatly separated in frequency. This is due to the convolution of the Fourier transform of the window with the signal, and agrees with what was predicted by Eq. 17: indeed windows with a larger main lobe exhibit a larger "radius" (bandwidth) in which the error of the parameter estimation will be high. However, for signals where local inner-product maxima are from atoms sufficiently separated in frequency, windows with lower sidelobes are better at attenuating the other component and for these the estimation error is lowest.

8. CONCLUSIONS

Motivated by the need to analyse mixtures of frequency- and amplitude-modulated sinusoids (Eq. 3), we have shown that the DDM can be employed under a single-component assumption when components have roughly disjoint sets of atoms for which their inner products take on large values. This indicates the need for windows whose Fourier transform exhibits low sidelobes. We developed windows whose sidelobes are minimized while remaining everywhere once-differentiable: a requirement to generate valid atoms for the DDM. These windows were shown to only improve parameter estimation of $P = 1$ component with argument-polynomial of order $Q = 2$ in low amounts of noise. However, for $P = 2$ components of the same order in mixture without noise, granted the

components exhibited reasonable separation in frequency between the atoms for which the inner product was maximized, these new windows substantially improved the estimation of all but the first argument-polynomial coefficient.

Further work should evaluate these windows on sinusoids of different orders, i.e., $Q \gg 1$. Optimal main-lobe widths for windows should be determined depending on the separation of local maxima in the power spectrum. It should also be determined if these windows improve the modeling of real-world acoustic signals.

9. ACKNOWLEDGMENTS

This work was partially supported by grant from the Natural Sciences and Engineering Research Council of Canada awarded to Philippe Depalle (RGPIN-262808-2012).

10. REFERENCES

[1] Michaël Betser, "Sinusoidal polynomial parameter estimation using the distribution derivative," *IEEE Transactions on Signal Processing*, vol. 57, no. 12, pp. 4633–4645, 2009.

[2] Xavier Serra, *A system for sound analysis/transformation/synthesis based on a deterministic plus stochastic decomposition*, Ph.D. thesis, Stanford University, 1989.

[3] Sylvain Marchand and Martin Raspaud, "Enhanced time-stretching using order-2 sinusoidal modeling," in *Proceedings of the 7th International Conference on Digital Audio Effects (DAFx-04)*, 2004, pp. 76–82.

[4] Lippold Haken, Kelly Fitz, and Paul Christensen, "Beyond traditional sampling synthesis: Real-time timbre morphing using additive synthesis," in *Analysis, Synthesis, and Perception of Musical Sounds*, pp. 122–144. Springer, 2007.

[5] Robert J McAulay and Thomas F Quatieri, "Speech analysis/synthesis based on a sinusoidal representation," *IEEE Transactions on Acoustics, Speech and Signal Processing*, vol. 34, no. 4, pp. 744–754, 1986.

[6] Wen Xue, "Piecewise derivative estimation of time-varying sinusoids as spline exponential functions," in *Proceedings of the 19th International Conference on Digital Audio Effects (DAFx-16)*, 2016, pp. 255–262.

[7] Brian Hamilton and Philippe Depalle, "A unified view of non-stationary sinusoidal parameter estimation methods using signal derivatives," in *the proceedings of the 2012 IEEE International Conference on Acoustics, Speech and Signal Processing (ICASSP)*. IEEE, 2012, pp. 369–372.

[8] Dan Stowell, Sašo Muševič, Jordi Bonada, and Mark D Plumbley, "Improved multiple birdsong tracking with distribution derivative method and Markov renewal process clustering," in *the proceedings of the 2013 IEEE International Conference on Acoustics, Speech and Signal Processing (ICASSP)*. IEEE, 2013, pp. 468–472.

[9] Elliot Creager, "Musical source separation by coherent frequency modulation cues," M.A. thesis, McGill University, 2016.

[10] Brian Hamilton and Philippe Depalle, "Comparisons of parameter estimation methods for an exponential polynomial sound signal model," in *Audio Engineering Society Conference: 45th International Conference on Applications of Time-Frequency Processing in Audio*. Audio Engineering Society, 2012.

[11] Axel Röbel, "Estimating partial frequency and frequency slope using reassignment operators," in *International Computer Music Conference*, 2002, pp. 122–125.

[12] Laurent Schwartz and Institut de mathématique (Strasbourg), *Théorie des distributions*, vol. 2, Hermann Paris, 1959.

[13] Steven M Kay, *Fundamentals of statistical signal processing, volume I: Estimation theory*, Prentice Hall, 1993.

[14] Jont B Allen and Lawrence R Rabiner, "A unified approach to short-time Fourier analysis and synthesis," *Proceedings of the IEEE*, vol. 65, no. 11, pp. 1558–1564, 1977.

[15] Albert Nuttall, "Some windows with very good sidelobe behavior," *IEEE Transactions on Acoustics, Speech, and Signal Processing*, vol. 29, no. 1, pp. 84–91, 1981.

[16] Fredric J Harris, "On the use of windows for harmonic analysis with the discrete Fourier transform," *Proceedings of the IEEE*, vol. 66, no. 1, pp. 51–83, 1978.

[17] L Rabiner, Bernard Gold, and C McGonegal, "An approach to the approximation problem for nonrecursive digital filters," *IEEE Transactions on Audio and Electroacoustics*, vol. 18, no. 2, pp. 83–106, 1970.

[18] Gene H Golub and Charles F Van Loan, *Matrix computations*, The John Hopkins University Press, 3rd edition, 1996.

[19] David Slepian, "Prolate spheroidal wave functions, Fourier analysis, and uncertainty V: The discrete case," *Bell Labs Technical Journal*, vol. 57, no. 5, pp. 1371–1430, 1978.

[20] Tony Verma, Stefan Bilbao, and Teresa HY Meng, "The digital prolate spheroidal window," in *the proceedings of the 1996 IEEE International Conference on Acoustics, Speech, and Signal Processing (ICASSP)*. IEEE, 1996, vol. 3, pp. 1351–1354.

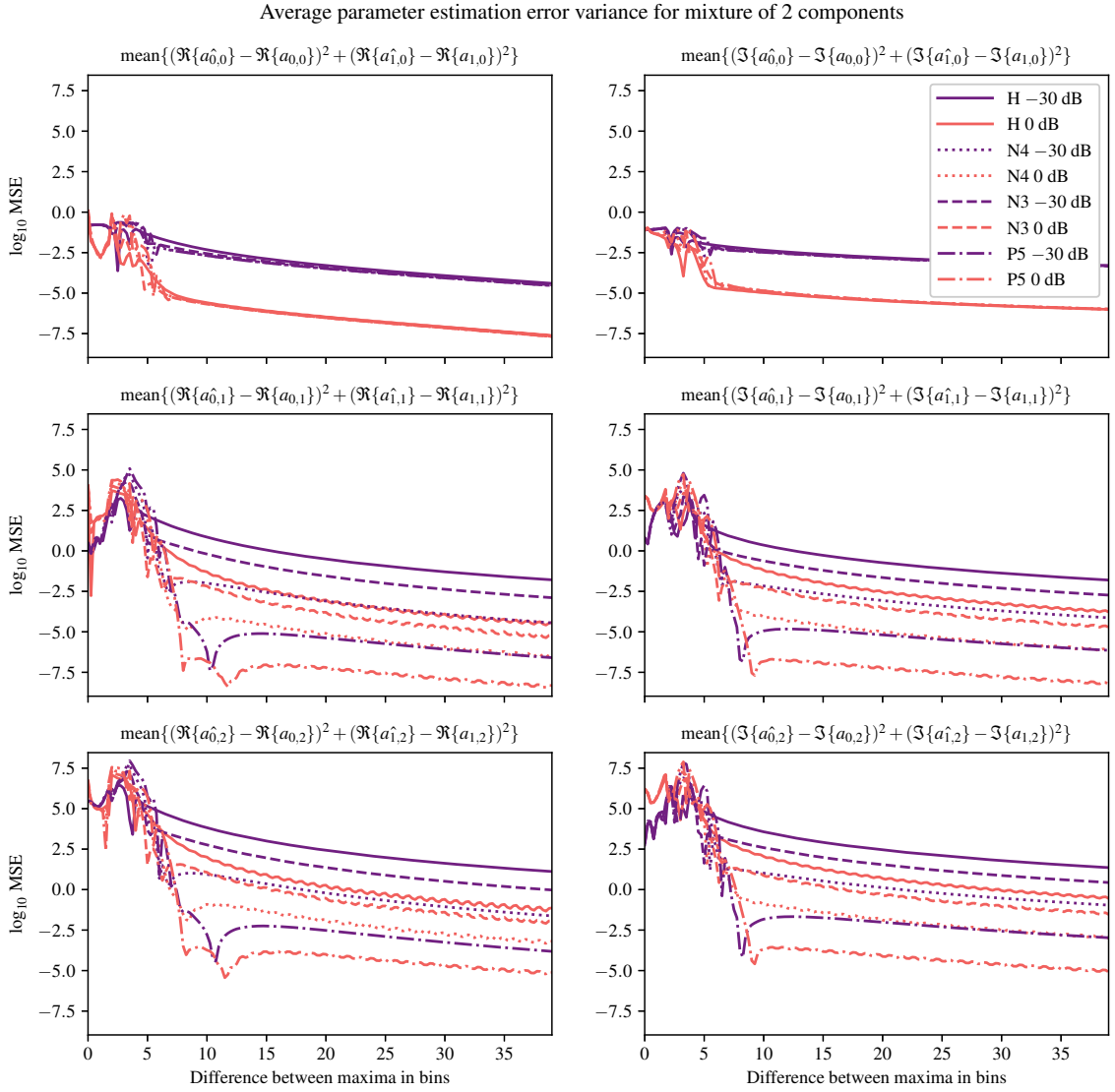

Figure 3: The mean squared estimation error for each parameter in an analysis of two components in mixture. A set of $K_2 = 10$ chirps was synthesized and each unique pair used for maximum bin differences $0 \leq d < 40$, with d varied in 0.25 bin increments. The signal power ratio between components is indicated with colours and the corresponding ratio in decibels is indicated in the plot legend. The names indicate the windows used to generate the atoms for estimation: *N3* and *N4* are the 3- and 4-cosine-term continuous Nuttall windows, *H* is the Hann window, and *P5* is the continuous 5-cosine-term approximation to a digital prolate window as described in Sec. 6.